

Crystal Structure and Thermodecomposition Kinetics of Copper(II) Ternary Complex with *o*-Vanillin-aurine Schiff-base and 1,10-Phenanthroline†

LI-RONG YANG, CAI-FENG BI*, YU-HUA FAN, SI-QUAN LU,
FENG GUO and XIAO-KANG AI

College of Chemistry and Chemical Engineering
Ocean University of China, Qingdao, 266003, China

Fax: (86)(532)82032483; E-mail: befeng@ouc.edu.cn, lirongyang_2005@yahoo.com.cn

A complex of copper(II) with *o*-vanillin-aurine Schiff base and 1,10-phenanthroline (1,10-phen) ($C_{22}H_{25}CuN_3O_8S$, $M_r = 555.05$), has been synthesized and characterized by IR, elemental analysis and X-ray diffraction single crystal analysis. The crystal belongs to monoclinic, space group $P2(1)/c$ with $a = 14.8310(16)$ Å, $\alpha = 90.00^\circ$, $b = 26.580(3)$ Å, $\beta = 112.890(2)^\circ$, $c = 12.8486(14)$ Å, $\gamma = 90.00^\circ$, $V = 4666.2(9)$ Å³, $Z = 8$, $F(000) = 2296$, $D_c = 1.580$ g/cm³, $\mu = 1.080$ mm⁻¹. In the molecule, the Schiff base and 1,10-phen act as tridentate and bidentate ligands, respectively, to form a distorted triangle bipyramid geometry. The prominent feature of the complex is that taurine in the Schiff base offers SO_3^- as a donor. The thermal decomposition kinetics of the complex have been investigated under non-isothermal condition using the Achar differential method and the Coats-Redfern integral method. The kinetic equation (of step (3)) may be expressed as follows: $da/dt = A \cdot e^{(-E/RT)} \cdot 3/2[(1-a)^{-1/3} - 1]$, $E = 72.42$ kJ/mol, $\ln A = 14.70$.

Key Words: Crystal structure, Copper(II) ternary complex, Thermodecomposition kinetics.

INTRODUCTION

Transitional metal complexes of sulphur-containing amino acid Schiff bases attracted considerable attention in view of their physico-chemical properties and potentially therapeutic properties¹⁻³. Some Schiff-bases containing sulphur and their copper(II) complexes have been shown to display antifungal and antibacterial properties⁴. During the past few years, researches mainly focussed on the complexes of α -amino acid Schiff bases, whereas those of β -amino acid were less reported, especially the complexes of taurine⁵. The sulphonic acid analogue of β -alanine ($NH_2CH_2CH_2COOH$), taurine ($NH_2CH_2CH_2SO_3H$) plays a role in a

†CCDC-273720 contains the supplementary crystallographic data for this paper. These data can be obtained free of charge via www.ccdc.cam.ac.uk/data_request/cif or by emailing: data_request@ccdc.cam.ac.uk or by contacting: The Cambridge Crystallographic Data Centre, 12, Union Road, Cambridge CB2 1EZ, UK, Fax: (44)(1223)336033.

lot of physiological and pathological conditions and pharmacological actions including cardiovascular, central and membrane stabilization, as well as osmoregulation, antioxidant and anti-inflammatory effects⁶⁻⁸. Although taurine is a simple compound, there are only a few studies on its behaviour as a ligand to metals. This is probably due to the smaller affinity to metals and poor stability of its complexes⁹⁻¹¹. From values of the stability constants for complexes formed by taurine, it is confirmed that taurine is not able to form chelates¹². This is in agreement with Ahrland who asserted that the SO_3^- group has few possibilities to be an electron donor and therefore the formation of chelate is most improbable¹³.

The aim of this research is to investigate the complex of taurine as a ligand chemically modified by the formation of Schiff base, followed by the studies of its structures and bioactivities. Consequently, the title complex was synthesized; its crystal structure and thermodecomposition kinetics are reported.

EXPERIMENTAL

Elemental analyses were performed on Perkin-Elmer 240C elemental analyzer. IR spectra were recorded in the $4000\text{--}400\text{ cm}^{-1}$ region, using KBr pellets on an Avatar 360 FT-IR spectrometer and crystal structures were determined on Smart CCD diffractometer. The thermogravimetric measurements were made using a Perkin-Elmer TGA7 thermogravimeter. The heating rate was programmed to be $10^\circ\text{C}/\text{min}$ with the protecting stream of N_2 flowing at $40\text{ mL}/\text{min}$.

Preparation of the complex: All chemicals were of analytical reagent grade and used directly without further purification.

Taurine and potassium hydroxide (0.01 mol) were added (with stirring) to anhydrous ethanol (20 mL) to make a pellucid solution. Then, it was slowly dripped into the anhydrous ethanol solution (15 mL) containing 0.01 mol *o*-vanillin at 40°C . The mixture was stirred for 0.5 h to give a golden clear solution. When cooled down to room temperature, a mass of golden grains separated out. The product, namely, *o*-vanillin taurine Schiff base, was collected by filtration and washed several times with anhydrous ethanol and dried under vacuum for later use. Yield 91.2%. Anal. (%), Calcd. for $\text{C}_{10}\text{H}_{12}\text{NSO}_3\text{K}\cdot\text{H}_2\text{O}$: C, 42.38; H, 4.98; N, 4.94; S, 11.32; Found: C, 42.01; H, 4.49; N, 5.15; S, 11.85. IR (KBr, cm^{-1}): 1639.2 $\nu(\text{C}=\text{N})$, 1252.0, 1208.9, 1054.3 and 966.0 $\nu(\text{SO}_3^-)$.

Cupric acetate (0.5 mmol) in 15 mL of methanol was added dropwise into the solution of Schiff-base (the same molar ratio with the anterior) in 15 mL of methanol and was stirred at 50°C . After 2 h, 10 mL of anhydrous ethanol containing 0.5 mmol 1,10-phen was dripped into the mixture, continuously to be stirred at the same temperature for 8 h. The dark green solution obtained was filtered and the filtrate was left for slow evaporation at room temperature. The dark green slantwise prism crystals formed after 10 days. Anal. (%), Calcd. for $\text{C}_{22}\text{H}_{25}\text{CuN}_3\text{O}_8\text{S}$: C, 47.60; H, 4.54; N, 7.57; S, 5.78; Found: C, 47.21; H, 4.39; N, 7.71; S, 5.84. IR (KBr, cm^{-1}): 3452.1 $\nu(\text{O}-\text{H})$, 1620.2 $\nu(\text{C}=\text{N})$, 1248.0, 1181.7, 1039.4 and 975.4 $\nu(\text{SO}_3^-)$, 456.6 $\nu(\text{Cu}-\text{O})$, 406.7 $\nu(\text{C}-\text{N})$.

X-Ray crystallographic determination: The selected crystal of dimensions $0.43 \times 0.38 \times 0.34$ mm was mounted on a Bruker Smart CCD X-ray single-crystal diffractometer. Reflection data were at 293(2) K using graphite monochromated MoK α radiation ($\lambda = 0.71073$), ω -2 θ scan mode. A total of 7574 independent reflections were collected in the range of $12.88^\circ \leq \theta \leq 25.10^\circ$, of which 5395 reflections with $I > 2\sigma(I)$ were considered to be observed and used in the subsequent refinement. Intensities were corrected for Lorentz and polarization effects and empirical absorption and the data reduction using SADABS program¹⁴.

The structure was solved by direct methods using SHELXS-97¹⁵. Positional and thermal parameters were refined by full-matrix least-squares method using the SHELXTL software package¹⁶. The final least-square cycle of refinement gave $R = 0.0782$, $wR = 0.1710$, the weighting scheme $w = 1/\sigma^2(F_0^2) + (0.1083P)^2 + 0.0000P$, where $P = (F_0^2 + 2F_c^2)/3$. A summary of the key crystallographic information is given in Table-1.

TABLE-1
SUMMARY OF CRYSTALLOGRAPHIC DATA FOR THE COMPLEX

Empirical formula	C ₂₂ H ₂₅ CuN ₃ O ₈ S	Crystal size (mm ³)	0.43 × 0.38 × 0.34
Formula weight	555.05	Range for data collection (°)	1.88–25.10
Temperature (K)	293(2)	Limiting indices	–17 ≤ h ≤ 17, –31 ≤ k ≤ 31 –15 ≤ l ≤ 10
Wavelength (Å)	0.71073		
Crystal system	Monoclinic		
Space group	P2(1)/c	Reflections collected/unique	21988/7574 [R _{int} = 0.0653]
a (Å)	14.8310(16)	Refinement method	Full-matrix least squares on F ²
b (Å)	26.580(3)	Data / restraints / parameters	7574 / 84 / 699
c (Å)	12.8486(14)	Goodness-of-fit on F ²	1.034
α (°)	90.00	Final R indices [I > 2σ(I)]	R ₁ = 0.0782, wR ₂ = 0.1710
β (°)	112.890(2)		
γ (°)	90.00		
Volume (Å ³)	4666.2(9)	R indices (all data)	R ₁ = 0.1106, wR ₂ = 0.1494
F(000)	2296	Largest diff. peak and hole (e · Å ⁻³)	0.656 and –0.472

RESULTS AND DISCUSSION

Description of crystal structure: Non-hydrogen fractional atomic coordinates and equivalent isotropic displacement parameters, selected bond lengths and angles and hydrogen bond distances of the complex are listed in Tables 2–4, respectively. An ORTEP drawing of the structure around copper(II) with the atom numbering scheme is shown in Fig. 1 and the packing drawing of the complex in Fig. 2.

TABLE-2
NON-HYDROGEN FRACTIONAL ATOMIC COORDINATES ($\times 10^4$) AND
EQUIVALENT ISOTROPIC DISPLACEMENT PARAMETERS ($\text{\AA}^2 \times 10^3$)

Atom	x	y	z	U(eq)	Atom	x	y	z	U(eq)
Cu(1)	8520(1)	5392(1)	2324(1)	57(1)	N(5)	3377(3)	6856(2)	6388(4)	36(1)
Cu(2)	4265(1)	6401(1)	5803(1)	37(1)	N(6)	2991(3)	6377(2)	4443(4)	39(1)
N(1)	7141(4)	5585(2)	1851(5)	51(1)	O(1)	8174(3)	4817(2)	1361(5)	68(1)
N(2)	9067(4)	5693(2)	3933(5)	61(2)	O(3)	8723(4)	6056(2)	1332(6)	104(2)
N(3)	9947(4)	5211(2)	2828(6)	63(2)	O(6)	4366(3)	5684(1)	5757(3)	43(1)
N(4)	5542(3)	6484(2)	7011(4)	34(1)	O(8)	4729(3)	6913(2)	4749(4)	56(1)

$$U_{eq} = (1/3) \sum_i \sum_j U_{ij} a_i^* a_j^* a_i a_j$$

TABLE-3
SELECTED BOND LENGTHS (\AA) AND ANGLES ($^\circ$)

Bond	Dist.	Bond	Dist.	Bond	Dist.
Cu(1)-O(1)	1.907(5)	Cu(1)-N(2)	2.066(7)	Cu(2)-N(6)	2.014(4)
Cu(1)-O(3)	2.265(6)	Cu(1)-N(3)	2.016(5)	O(3)-S(1)	1.454(6)
Cu(2)-O(6)	1.914(3)	Cu(2)-N(4)	1.939(4)	O(4)-S(1)	1.461(8)
Cu(2)-O(8)	2.210(4)	Cu(2)-N(5)	2.129(4)	O(5)-S(1)	1.33(2)
Cu(1)-N(1)	1.961(5)				
O(1)-Cu(1)-N(1)	91.3(2)	N(1)-Cu(1)-O(3)	88.4(2)	N(4)-Cu(2)-N(5)	101.41(18)
O(1)-Cu(1)-N(3)	90.1(2)	N(3)-Cu(1)-O(3)	90.8(2)	N(6)-Cu(2)-N(5)	79.86(19)
N(1)-Cu(1)-N(3)	178.6(2)	N(2)-Cu(1)-O(3)	100.1(2)	O(6)-Cu(2)-O(8)	123.21(18)
O(1)-Cu(1)-N(2)	149.5(2)	O(6)-Cu(2)-N(4)	94.23(17)	N(4)-Cu(2)-O(8)	88.89(17)
N(1)-Cu(1)-N(2)	99.5(2)	O(6)-Cu(2)-N(6)	90.06(17)	N(6)-Cu(2)-O(8)	84.17(17)
N(3)-Cu(1)-N(2)	79.4(3)	N(4)-Cu(2)-N(6)	173.03(19)	N(5)-Cu(2)-O(8)	104.42(17)
O(1)-Cu(1)-O(3)	108.7(3)	O(6)-Cu(2)-N(5)	130.03(17)		

TABLE-4
HYDROGEN BOND DISTANCES (\AA) OF THE COMPLEX

D	H	A	symm.	D—H	H...A	D...A	D—H...A
O(11)-H(45)...		O(10')	x, -y + 3/2, z + 1/2	0.832	2.639	3.206	126.66
O(12)-H(48)...		O(10')	x, -y + 3/2, z + 1/2	0.834	2.288	2.738	114.25
O(13)-H(49)...		O(16)	x, -y + 3/2, z - 1/2	0.837	2.416	2.965	123.92
O(14)-H(51)...		O(1)	x, y, z + 1	0.861	2.087	2.889	154.80
O(14)-H(51)...		O(2)	x, y, z + 1	0.861	2.224	2.868	131.45
O(14)-H(52)...		O(15)		0.856	2.133	2.977	168.33
O(15)-H(53)...		O(16)		0.852	2.310	2.980	135.69
O(16)-H(55)...		O(13)	x, -y + 3/2, z + 1/2	0.861	2.436	2.965	120.34

Fig. 1 shows that the geometry of the complex $[\text{Cu}(o\text{-vanillin taurine})(1,10\text{-phen})] \cdot 3\text{H}_2\text{O}$ gives a triangle bipyramid with N(2) belonging to 1,10-phen- O(1) (deprotonated phenolic oxygen) and O(3) ($-\text{SO}_3^-$) belonging to Schiff base ligand

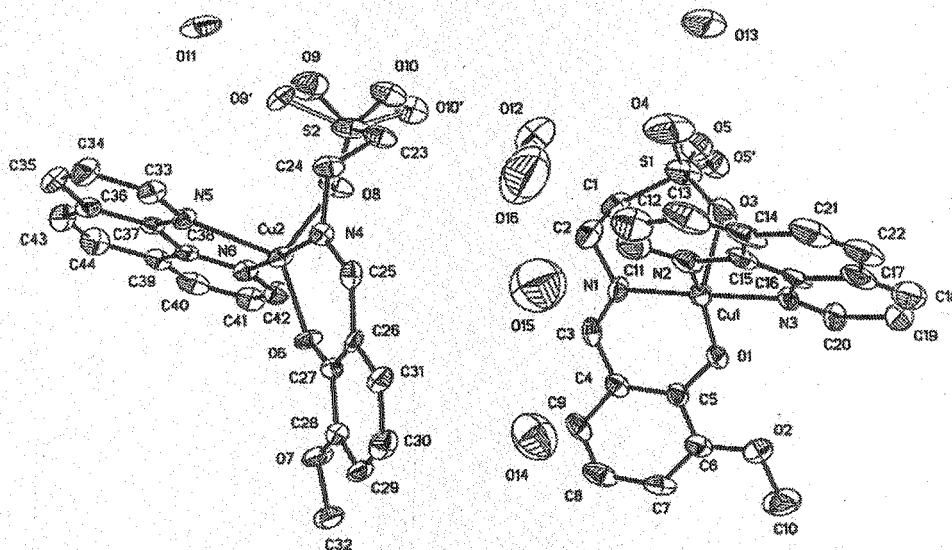


Fig. 1. Crystal structure of the complex

occupying each vertex of the equatorial site, while N(1) of Schiff base and N(3) of 1,10-phen located in the apical positions along the axis). The corresponding bond angles are: O(1)-Cu(1)-O(3) ($108.7(3)^\circ$), O(1)-Cu(1)-N(2) ($149.5(2)^\circ$), O(3)-Cu(1)-N(2) ($100.1(2)^\circ$) (Table-3); the sum of bond angles is 358.37° (nearly 360°), which indicates that the three atoms (O(1), O(3), N(2)) are almost coplanar under the experimental error. It can also be proved by the sum of the internal angles of the equator triangle (O(1)-N(2)-O(3) (56.12°), O(3)-O(1)-N(2) (54.31°) and O(1)-O(3)-N(2) (69.57°), summation: 180.00°). The bond distance of Cu(1)-N(1) is $1.961(5)$ Å (Table-3), which is significantly shorter than that of Cu(1)-N(3) ($2.016(5)$ Å). As can be seen from the bond angles and bond distances listed above (for example, O(1)-Cu(1)-N(2) ($149.5(2)^\circ$) is observably larger than that of the ideal one of 120° in normal triangle bipyramid), the coordination geometry of the Cu(II) atom is a slightly distorted triangle bipyramid. Another manifestation is the slight departure of the axis from the beeline (N(1)-Cu(1)-N(3) ($178.6(2)^\circ$)). Even Jahn-Teller distortions may play the concomitant role in Cu(II) ion.

Some bond distances of Cu-N (Cu(2)-N(4) ($1.939(4)$ Å), Cu(2)-N(5) ($2.129(4)$ Å) etc.) are in some sort different from those observed in the tetrahedral structures with an average of $2.082(6)$ ¹⁷ and a range of $1.991(2)$ – $2.105(2)$ Å^{18, 19}. Steric hindrance imposed by the conjugated aryl-ring of 1,10-phen in [Cu(*o*-vanillin taurine) (1,10-phen)]·3H₂O, leads to lengthening of the Cu(1)-N(2) ($2.066(7)$ Å). Bond distances between 1,10-phen and Cu(II) (Cu(1)-N(2), Cu(1)-N(3)) are markedly longer than those between Schiff base and Cu(II) (Cu(1)-N(1), Cu(1)-O(1)), with the exception of O(3)-Cu(1) ($2.265(6)$ Å), suggesting that the coordination ability of Schiff base is stronger than that of 1,10-phen; in addition, O(1) (deprotonated phenolic oxygen) is stronger than O(3) (—SO₃⁻). In the complex, O(3) (—SO₃⁻) acts as a new donor, owing to the change of steric hindrance and the redistribution of charge intensity of O atoms after the formation of *o*-vanillin taurine Schiff base.

Fig. 2 illustrates that hydrogen bonds occur between water molecules (O(14)-H(52)···O(15), O(15)-H(53)···O(16) etc. (see Table-4) and between water mole-

cules and the complex molecules (O(14)-H(51)···O(1), O(14)-H(51)···O(2)) as well, which stabilized the crystal structure. Some distances between O atoms in the hydrogen bonds (O(15)···O(16) (2.302 Å), O(9)···O(11) (2.755 Å) and O(10)···O(14) (2.738 Å) etc.) are shorter than that of ice (2.76 Å) and pure water (2.83 Å)²⁰, which elucidates that water molecules are tightly connected among the crystal lattice.

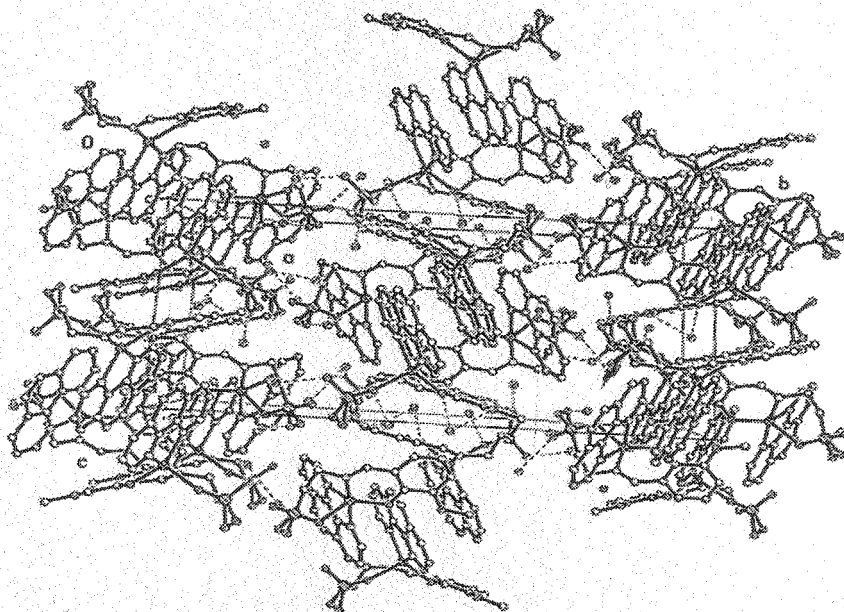


Fig. 2. Packing drawing of the complex

Spectroscopic studies: After the coordination, the characteristic absorption peaks of $-\text{SO}_3^-$ (1252.0, 1208.9, 1054.3 and 966.0 cm^{-1}) shift to 1248.0, 1181.7, 1039.4 and 975.4 cm^{-1} , which indicate that $-\text{SO}_3^-$ participated in the coordination. The band of $\nu(\text{C}=\text{N})$ shifts from 1639.2 to 1620.2 cm^{-1} , suggesting that the N atom in Schiff base is a donor. Vibrations of 1,10-phen at 1545.1 cm^{-1} split into 1552.1 and 1478.6 cm^{-1} , in-plane bending vibrations shift from 845.1 and 741.6 cm^{-1} to 818.4 and 739.6 cm^{-1} , respectively. A broad absorption band centres around 3452.1 cm^{-1} confirming the presence of crystalline water involved in hydrogen bonds. The bands appearing at 456.6 and 406.7 cm^{-1} attribute to $\nu(\text{C}-\text{O})$ and $\nu(\text{C}-\text{N})$ stretching vibrations are observed. These changes could be diagnostic for coordinated $[\text{Cu}(o\text{-vanillin taurine})(1,10\text{-phen})]\cdot 3\text{H}_2\text{O}$ complex.

Thermal decomposition kinetics studies: The TG and DTG curves of the complex are shown in Fig. 3, which indicate that the complex decomposes in three steps. The first and the second weight loss stages have decomposition temperature ranges of $25\text{--}110^\circ\text{C}$ and $110\text{--}260^\circ\text{C}$, with weight losses of 6.76% (calcd. 6.49%) and 2.92% (calcd. 3.06%), which corresponds to the losses of two molecules and one molecule of water, respectively. The fact suggests that water is close bound to the complex by hydrogen bonds which can be certified by the crystal structure diffraction simultaneously. The third weight loss stage has a decomposition temperature range of $260\text{--}800^\circ\text{C}$, corresponding to the losses of one molecule of Schiff base and one molecule of 1,10-phen (exothermic peaks

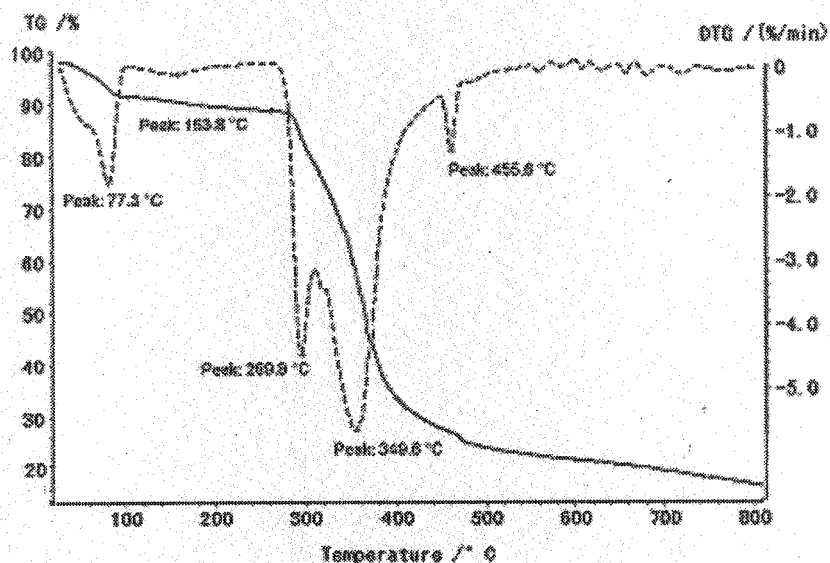
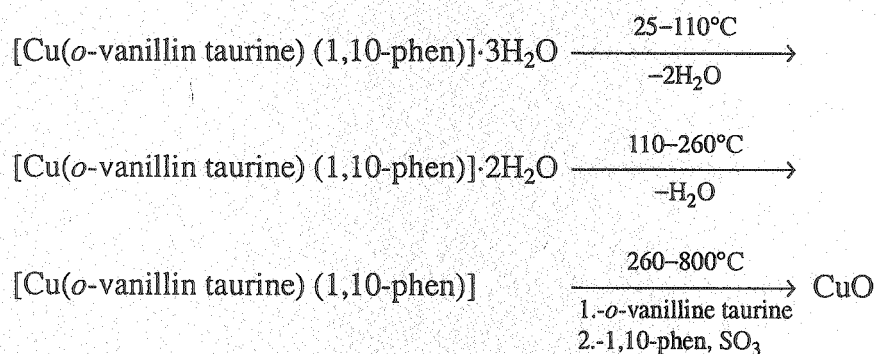


Fig. 3. TG-DTG curves of the complex

located in 289.8°C and 349.6°C, respectively). The fact that *o*-vanillin-aurine Schiff base was lost prior to 1,10-phen suggests that it is more sensitive to temperature than the latter. The weight percentage of 14.30% (calcd. 14.33%) of the original sample remained; CuO is the final residue. The process of thermal decomposition of the title complex may be shown as follows:



On the basis of 30 kinetic functions in both differential and integral forms commonly used in recent reports^{21, 22}, the non-isothermal kinetics of the step was investigated using the Achar differential method²³ and the Coats-Redfern integral method²⁴.

The original kinetic data for step (3) obtained from the TG and DTG curves are listed in Table-5, in which T^i is the temperature at any point i on the TG and DTG curves, a_i is the corresponding decomposition rate. $(da/dt)_i = [\beta/(W_0 - W_i)] \times (dW/dT)_i$ in which $(dW/dT)_i$ is the height of the peak in the DTG curve, β is the heating rate, and W_0 and W_1 are the initial and final weights at the stage, respectively.

The calculated kinetic parameters (E , A) and correlation coefficients (r) of step 3 are listed in Table-6.

TABLE-5
DATA FOR STEP (3) OF THE THERMODECOMPOSITION OF
THE COMPLEX OBTAINED FROM THE TG AND DTG CURVES

T_i (K)	a_i	$(da/dt)_i$
596	0.1145	0.0445
606	0.2576	0.0552
611	0.3371	0.0618
616	0.3603	0.0672
619	0.4768	0.0687
621	0.5130	0.0689
622	0.5309	0.0693
623	0.5485	0.0696
624	0.5667	0.0692
625	0.5848	0.0688
627	0.6027	0.0684
630	0.6741	0.0661
635	0.7562	0.0554
640	0.7650	0.0450
650	0.9316	0.0328
660	0.9999	0.0129

TABLE-6
RESULTS OF THE ANALYSIS OF THE DATA FOR STEP 3 IN TABLE-5 BY THE ACHAR
DIFFERENTIAL METHOD AND THE INTEGRAL METHOD (COATS-REDFERN)

	E (kJ/mol)	ln A	r	E (kJ/mol)	ln A	r
1.	15.98	2.56	0.4127	60.13	7.48	0.9232
2.	44.65	12.19	0.9017	70.71	10.67	0.9519
3.	65.83	18.20	0.9553	76.30	11.19	0.9650
4.	100.98	30.69	0.9137	89.52	15.95	0.9836
5.	5.75	-3.58	0.1670	52.90	2.50	0.9093
6.	206.44	68.19	0.8309	159.83	40.95	0.9335
7.	88.43	28.75	0.7580	55.80	7.20	0.9787
8.	67.87	21.37	0.6818	35.24	0.22	0.9764
9.	57.59	17.59	0.6287	24.96	-3.27	0.9378
10.	47.31	13.70	0.5619	14.68	-6.76	0.9669
11.	42.17	11.66	0.5223	9.54	-8.50	0.9569
12.	35.70	9.31	0.7716	37.01	-0.22	0.9671
13.	53.28	15.15	0.7663	41.82	1.11	0.9810
14.	-17.03	-8.74	0.5871	27.13	-3.13	0.9069
15.	-33.53	-14.74	0.8819	10.62	-8.43	0.8570
16.	-39.03	-16.91	0.9238	5.12	-10.20	0.7646

	E (kJ/mol)	ln A	r	E (kJ/mol)	ln A	r
17.	-41.78	-18.09	0.9388	2.37	-11.09	0.5858
18.	193.90	66.25	0.7488	132.59	34.37	0.8340
19.	141.16	46.81	0.7519	46.85	5.01	0.6996
20.	-28.03	-12.68	0.8177	16.13	-6.66	0.8855
21.	150.11	50.38	0.8672	117.48	28.13	0.9806
22.	211.79	71.72	0.9097	179.16	49.07	0.9812
23.	273.47	92.94	0.9308	240.84	70.00	0.9815
24.	299.36	104.43	0.7457	205.05	61.25	0.7302
25.	62.07	17.99	0.7638	44.70	1.85	0.9851
26.	-122.49	45.54	0.7224	16.14	-6.54	0.7712
27.	-227.95	-82.63	0.7306	9.97	-8.51	0.6331
28.	-333.41	-119.84	0.7335	6.06	-9.78	0.4913
29.	29.43	7.04	0.5465	17.97	-6.31	0.9737
30.	27.45	5.97	0.6655	15.56	-6.98	0.9530

The results obtained from the two different methods are approximately the same when based on function No. 3 for step 3, which corresponds to the mechanisms of the Ginstling-Brunshstein equation. The kinetic equation is expressed as follows:

$$\frac{da}{dt} = A \cdot e^{-E/RT} \cdot \frac{3}{2} [(1-a)^{-1/3} - 1]^{-1}, \quad E = 72.42 \text{ kJ/mol}, \quad \ln A = 14.70.$$

The activation entropy ΔS^\ddagger and activation free-energy ΔG^\ddagger are calculated by the following equations²⁵:

$$A = \frac{kT_P^\ddagger}{h} \exp\left(\frac{\Delta S^\ddagger}{R}\right), \quad Ae^{-E/RT} = \frac{kT_P^\ddagger}{h} \exp\left(\frac{\Delta S^\ddagger}{R}\right) \exp\left(-\frac{\Delta H^\ddagger}{RT}\right),$$

$$\Delta G^\ddagger = \Delta H^\ddagger - T \Delta S^\ddagger$$

in which T_P is the temperature at the top of peak (3), k is Boltzmann constant, R is gas constant, h is Planck's constant. The activation entropy ΔS^\ddagger and activation free-energy ΔG^\ddagger for the third thermal decomposition stage were obtained,

$$\Delta S^\ddagger = -128.82 \text{ J/mol} \cdot \text{K}, \quad \Delta G^\ddagger = 5.51 \text{ kJ/mol}.$$

Conclusions

This paper contributes to the investigations of the behaviour of taurine as a ligand modified by Schiff base towards copper(II). In our work, *o*-vanillin taurine Schiff base has been synthesized, which changes the steric and electronic effects and the basicity of SO_3 -group; consequently, its coordination ability is enhanced that favours the coordination with copper(II). The prominent feature of the complex is that taurine acts as a bidentate comparing to those reported in literature. The thermal decomposition kinetics of the complex are obtained using the Achar differential method and the Coats-Redfern integral method. The decomposition kinetic equation for the third step is:

$$\frac{da}{dt} = A \cdot e^{-E/RT} \cdot \frac{3}{2} [(1-a)^{-1/3} - 1]^{-1}, \quad E = 72.42 \text{ kJ/mol}, \quad \ln A = 14.70.$$

$$\Delta S^\ddagger = -128.82 \text{ J/mol} \cdot \text{K}, \quad \Delta G^\ddagger = 5.51 \text{ kJ/mol}.$$

Further researches on its binding to DNA by intercalation, antifungal and antibacterial bioactivities are proceeding recently.

REFERENCES

1. A.M. Akbar, T.S. Guan, P. Bhattacharjee, R.J. Butcher, J.P. Jasinski and Li Yu, *Trans. Met. Chem.*, **21**, 351 (1996).
2. A. Abu-Raqabah, G. Davies, M.A. El-Sayed, A. El-Toukhy, S.N. Shaikh and Zubeita, *Inorg. Chim. Acta*, **193**, 43 (1992).
3. A.M. Akbar, M. Nazimuddin, R. Shaha, J.R. Butcher and C.J. Bryan, *Polyhedron*, **17**, 3955 (1998).
4. M.E. Hossain, M.N. Alam, A.M. Akbar, M. Nazimuddin, J. Begum, F.E. Smith and R.C. Hynes, *Inorg. Chim. Acta*, **249**, 207 (1996).
5. S.K. Chandra, P. Basu, D. Ray, S. Pal and A. Chakravorty, *Inorg. Chem.*, **29**, 2423 (1990).
6. R.J. Huxtable, *Physiol. Rev.*, **72**, 101 (1992).
7. R.J. Huxtable and L.A. Sebring, *Drug Evaluation Reports: The Junior Class Project*, Trends Pharmacol. Sci., p. 480 (1986).
8. C.O. Eimear, F. Etelka, R. Antal and B.N. Kevin, *J. Inorg. Biochem.*, **77**, 135 (1999).
9. A.E. Martell and L.G. Sillen, *Stability Constants*, Special Publications, The Chemical Society, London, p. 25 (1971).
10. L.D. Pettit and H.K. Powell, IUPAC, *Stability Constants: Database*, Academic Software, Timble, Otley, Yorks, UK (1993).
11. F. Giorgio, F. Adamo, A. Giuseppe, R. Aldo and Z. Peter, *Microchem. J.*, **55**, 382 (1997).
12. B. Emilio, R.F. Maria, E. Bottari and M.R. Festa, *Talanta*, **46**, 91 (1998).
13. S. Ahrland, J. Chatt, N.R. Davies and A.A. Williams, *J. Chem. Soc.*, 264 (1954).
14. G.M. Sheldrick, SHELXTL 5, The Complete Software Package for Single Crystal Structure Determination, Siemens, AG, Analytical Systems Aut37, D76181 Karlsruhe 21, Germany (1995).
15. G.M. Sheldrick, SHELXTL 97, Program for Crystal Structure Refinement, University of Göttingen, Germany, 1997.
16. G.M. Sheldrick, SHELXTL 5, Reference Manual, Siemens Analytical X-ray Systems, Inc., Wisconsin, USA (1996).
17. H.Y. Sun, L.F. Bao, T. Okamura, W.X. Tang and N. Ueyama, *Eur. J. Inorg. Chem.*, **7**, 1855 (2001).
18. H.K. Fun, S.S.S. Raj, R.G. Xiong, J.L. Zuo, Z. Yu, X.L. Zhu and You X.Z., *J. Chem. Soc., Dalton Trans.*, **11**, 1711 (1999).
19. F.F. Jian, G.Y. Liu, Q.L. Hao and X. Wang, *Chinese J. Inorg. Chem.*, **19**, 419 (2003).
20. R.G. Xiong, C.M. Liu, J.L. Zuo, H.Z. Li, X.Z. You, H.K. Fun and K. Sivakumar, *Polyhedron*, **16**, 2315 (1997).
21. Z.L. Yu, *Thermal Analysis*, 1st Edn., Qinghua University Press, Beijing, p. 94 (1987).
22. Y.H. Fan, C.F. Bi and J.Y. Li, *Synth. React. Inorg., Met.-Org. Chem.*, **33**, 137 (2003).
23. B.N. Achar, *Proceeding International Clay Conference*, Book 1, Jerusalem, p. 67 (1966).
24. A.W. Coats and J.P. Redfern, *Nature (London)*, **201**, 68 (1964).
25. Z.H. Rong and S.Q. Zhen, *Thermal Analysis Kinetics*, Science Press, Beijing, p. 206 (2001).